

UNCLASSIFIED

Defense Technical Information Center
Compilation Part Notice

ADP022398

TITLE: Singular Grain Boundaries in Alumina and Their Roughening Transition

DISTRIBUTION: Approved for public release, distribution unlimited

This paper is part of the following report:

TITLE: Journal of the American Ceramic Society, Volume 86, Number 4.
Special Topical Issue: Alumina

To order the complete compilation report, use: ADA452328

The component part is provided here to allow users access to individually authored sections of proceedings, annals, symposia, etc. However, the component should be considered within the context of the overall compilation report and not as a stand-alone technical report.

The following component part numbers comprise the compilation report:

ADP022388 thru ADP022419

UNCLASSIFIED

Singular Grain Boundaries in Alumina and Their Roughening Transition

Chan Woo Park

Wireless Communication Devices Department, Basic Research Laboratory,
Electronics and Telecommunications Research Institute, Daejeon 305-350, Korea

Duk Yong Yoon*

Department of Materials Science and Engineering, Korea Advanced Institute of Science and Technology,
Daejeon 305-701, Korea

John E. Blendell* and Carol A. Handwerker*

Materials Science and Engineering Laboratory, National Institute of Standards and Technology,
Gaithersburg, Maryland 20899

The shapes and structures of grain boundaries formed between the basal (0001) surface of large alumina grains and randomly oriented small alumina grains are shown to depend on the additions of SiO₂, CaO, and MgO. If a sapphire crystal is sintered at 1620°C in contact with high-purity alumina powder, the grain boundaries formed between the (0001) sapphire surface and the small alumina grains are curved and do not show any hill-and-valley structure when observed under transmission electron microscopy (TEM). These observations indicate that the grain boundaries are atomically rough. When 100 ppm (by mole) of SiO₂ and 50 ppm of CaO are added, the (0001) surfaces of the single crystal and the elongated abnormal grains form flat grain boundaries with most of the fine matrix grains as observed at all scales including high-resolution TEM. These grain boundaries, which maintain their flat shape even at the triple junctions, are possible if and only if they are singular corresponding to cusps in the polar plots of the grain boundary energy as a function of the grain boundary normal. When MgO is added to the specimen containing SiO₂ and CaO, the flat (0001) grain boundaries become curved at all scales of observation, indicating that they are atomically rough. The grain boundaries between small matrix grains also become defaceted and hence atomically rough.

I. Introduction

SINCE the initial proposal by Burton, Cabrera, and Frank,¹⁻³ disordering of crystal surface has been extensively studied both theoretically and experimentally.⁴⁻⁷ A singular surface is atomically flat with a finite step free energy and corresponds to a cusp in the polar plot of the surface energy against the surface normal. A surface roughening transition occurs with either temperature increase or composition change when the step free energy becomes 0. Because the radius of a singular surface segment is proportional

to its step free energy,^{5,6} it becomes 0 when the roughening transition occurs. The roughening transition is thus characterized by the shape change from flat to curved. A crystal surface with an orientation which does not appear in the equilibrium shape can develop a hill-and-valley (h&v) shape^{3,8} and undergo defaceting transition with temperature increase or composition change. For example, the exposure of alumina surfaces with h&v shapes to MgO atmosphere was observed to induce the defaceting transition.⁹ Because the defaceting transition is usually equivalent to the rounding of the edges and corners of the equilibrium crystal shape, it implies an eventual roughening transition of the singular surface if the temperature or composition change proceeds further.

Following the initial proposal of Hart,¹⁰ the possibility of grain boundary transition has also been studied. Several molecular dynamics simulations^{11,12} showed gradual grain boundary disordering with temperature increase above about $0.5T_m$, where T_m is the melting point. By making an analogy to the surface roughening, Rottman¹³ showed that low-angle grain boundaries in Cu could undergo roughening transitions. Defaceting transitions with temperature increase¹⁴⁻¹⁷ and composition change^{18,19} have been observed in metals. Dahmen and Westmacott²⁰ observed a nearly polyhedral aluminum grain (embedded in another aluminum grain) developing rounded edges on heating to a high temperature and changing reversibly on cooling. There has also been indirect experimental evidence for grain boundary transitions from the measurements of grain boundary energy,²¹ sliding,²²⁻²⁴ and migration²⁵ at various temperatures. Thus, the grain boundary roughening transition appears to be very possible, but it has not yet been clearly demonstrated based on complete structural characterization.

As for crystal surfaces, the characteristics of grain boundaries are determined by the equilibrium shape of a grain (an island grain) embedded in another grain with a certain misorientation angle. The equilibrium shape of an island grain thus depends on the polar plot of the grain boundary energy against the grain boundary normal. By analogy with crystal surfaces,²⁶ the flat or curved grain boundary segments in the equilibrium shape will be singular or rough, respectively. The shapes of grain boundaries in polycrystals can thus be divided into three types. If a grain boundary is flat at all scales of observation (including HRTEM scales), it is likely to be singular. If a grain boundary is curved at all scales of observation, it is likely to be rough. A grain boundary can also have an h&v shape and the segments of such a boundary can be either singular or rough. Both flat boundaries and h&v boundaries have previously been referred to as faceted.

The purpose of this work is to examine the possibility that the flat grain boundaries between the basal (0001) planes of the abnormal

S. M. Wiederhorn—contributing editor

Manuscript No. 186772. Received August 15, 2002; approved November 18, 2002. Presented at the International Symposium on Science and Technology of Alumina (Schloss-Ringberg, Germany, March 17-22, 2002).

Supported by the Korea Ministry of Science and Technology through the National Research Laboratory (NRL) Program and by the Korea Ministry of Education through the Brain Korea 21 (BK21) Program.

*Member, American Ceramic Society.

grains and the randomly oriented planes of the small grains in contact, which form during abnormal grain growth (AGG) with small amounts of SiO_2 and CaO , are singular with cusps in the polar plots of the grain boundary energy γ against the boundary normal or the inclination angle. Such grain boundaries will be called the basal or the (0001) grain boundaries. While such grain boundaries are naturally formed by AGG, we also form them artificially by diffusion bonding the sapphire single crystals to small grains in powder form. We will also examine the possibility, by observing the shape changes at all scales, that these grain boundaries become rough when MgO is added.

If SiO_2 and CaO are present in alumina as additives or impurities, usually some grains grow abnormally during heat treatment and these large grains are often elongated along their basal planes forming flat boundaries with the neighboring fine grains.^{27–30} It has been suggested that such flat boundaries were formed because there were thin liquid layers between the basal planes of the large grains and the small neighboring grains.^{29,31} But flat grain boundaries can form in alumina without any liquid phase. For example, in a commercial-grade alumina doped with TiO_2 and MgO , Swiatnicki *et al.*³² found flat grain boundaries parallel to the basal (0001) or rhombohedral {01 $\bar{1}$ 2} planes of one of the grains with no amorphous phase at these boundaries as observed by high-resolution transmission electron microscopy (HRTEM). Gülgün *et al.*³³ also found similar flat grain boundaries in alumina doped with 1000 ppm (by mole) of yttrium and hot-pressed at 1475°C. Lartigue *et al.*³⁴ also observed grain boundaries lying on the basal planes in alumina codoped with MgO and Y_2O_3 . Park and Yoon³⁰ observed that the grain boundaries in alumina doped with small amounts of SiO_2 and CaO had h&v shapes and all of them became curved when doped with MgO . Although these defaceting transitions indicated that SiO_2 and CaO made the grain boundaries singular and MgO made them rough in alumina, they were not the direct observations of the roughening transitions. In this work, we will identify the basal grain boundaries as singular and observe their roughening transition from their shape changes. It should be noted that such a flat singular grain boundary parallel to the basal plane in one of the grain pairs can form for any misorientation angle between them.

Changes in interface equilibrium shape with temperature or composition can be made only if the interfaces are moving slowly compared with the rate at which structural changes occur along the interface. This is equivalent to the assumption of local equilibrium in phase transformations. It has been demonstrated that these conditions can be sometimes met for grain boundaries.²⁰

II. Experimental Procedure

The specimens were prepared from α -alumina powder of purity exceeding 99.998%. For the sources of SiO_2 and CaO , $\text{Si}(\text{OC}_2\text{H}_5)_4$ (>99.999%) and $\text{Ca}(\text{NO}_3)_2 \cdot x\text{H}_2\text{O}$ (>99.99%) were used. Alumina powder doped with 100 ppm of SiO_2 and 50 ppm of CaO (by mole) was prepared by mixing the pure alumina powder with the dopants in ethyl alcohol and drying at 70°C. This powder was the same as that used in our previous study of grain growth in pure alumina and alumina doped with 100 ppm of SiO_2 and 50 ppm of CaO (by mole) at 1620°C.³⁰

Commercially available α - Al_2O_3 (>99.996%) single-crystal disks with (0001) faces perpendicular to the disk axis were vertically cut into pieces with dimensions of 1 mm \times 2.5 mm \times 1 mm, and cleaned in a solution of HCl and HNO_3 . Each single-crystal piece was embedded in alumina powder, either pure or containing 100 ppm SiO_2 + 50 ppm CaO , pressed uniaxially into cylindrical compacts, and then pressed isostatically at 100 MPa. The compacts were heated at 950°C for 1 h to convert the dopant chemicals to oxides and to remove ethyl alcohol. The compacts were then sintered and heat-treated at 1620°C for 12 or 24 h in air in a high-purity alumina tube. The sintered specimens were sectioned to reveal the embedded single crystals, and the surfaces were polished with diamond pastes down to 0.25 μm and thermally etched at 1550°C for about 30 min for examination by scanning electron microscopy (SEM; Model 515, Philips, Holland). The specimens for transmission electron microscopy (TEM; JEM-3010, JEOL, Tokyo, Japan) were prepared by mechanical grinding and ion-beam milling.

To examine the effect of MgO on the shape of the grain boundaries already containing SiO_2 and CaO , a sintered specimen with SiO_2 and CaO was sliced into a piece about 1 mm thick and subsequently heat-treated in an alumina crucible packed with MgO powder (>99%) at 1620°C for 10 or 24 h. Grain boundary transitions with the addition of SiO_2 and CaO were also studied by heat-treating a slice of the specimen previously sintered with pure alumina powder embedded in alumina powder with 100 ppm SiO_2 + 50 ppm CaO .

III. Results and Discussion

The pure polycrystalline alumina in our previous work³⁰ showed normal grain growth with equiaxial grains in agreement with other observations.^{27,35–37} The grain boundaries had typical curved shapes. The contact region between the initially (0001) face of the single crystal and pure alumina powder is shown in Fig. 1(a) and the upper part shows a typical normal grain growth structure.

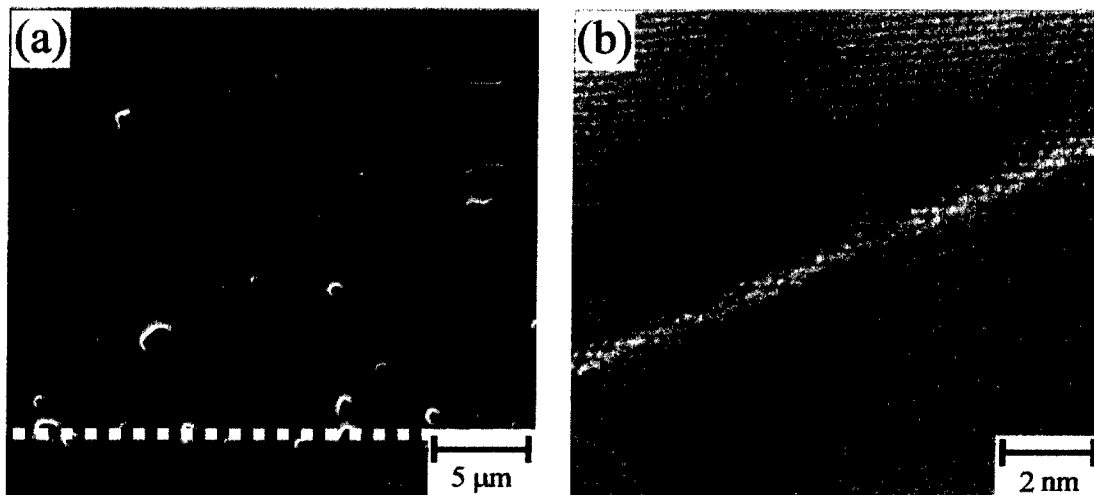


Fig. 1. (a) SEM image of the microstructure of the contact region between the (0001) face of a sapphire crystal and pure alumina powder sintered at 1620°C for 24 h, and (b) the HRTEM image of a grain boundary in pure alumina sintered at 1620°C for 12 h.

The grain boundaries formed between the single crystal and fine grains had moved from the initial position indicated by a dotted line along the pores. The grain boundaries between the fine matrix grains and between the matrix grains and the single crystal were curved as shown in Fig. 1(a). The TEM observations at intermediate magnifications also showed curved grain boundaries between the matrix grains without any flat or h&v shapes, as observed previously (see Fig. 1(b) in Ref. 30). The HRTEM images of these grain boundaries also showed curved boundaries which did not fall into any crystallographic plane of either or both grains, as exhibited in Fig. 1(b). Such curved shapes at all magnifications indicate that these grain boundaries are atomically rough (at the heat-treatment temperature of 1620°C). Although the grain boundaries between the single crystal and the matrix grains were not observed under TEM, their curved shapes at a relatively low magnification of Fig. 1(a) indicate that they are also atomically rough. (This will be confirmed below by TEM observations of similar grain boundaries in a specimen doped with MgO.)

The grain boundaries will have (local) equilibrium structures only if they are not moving or moving very slowly. The grain boundaries between the matrix grains in Fig. 1(a) were moving relatively slowly as indicated by the small average grain size difference between this specimen sintered for 24 h (6.9 μm) and that sintered for 12 h (6.5 μm) shown in our previous paper.³⁰ Therefore, the equilibrium structure of the grain boundaries in pure alumina is rough at 1620°C.

When a single crystal embedded in alumina powder containing 100 ppm of SiO_2 and 50 ppm of CaO was sintered, flat basal grain boundaries formed between the (0001) face of the single crystal and the matrix grains as shown in Fig. 2(a). In the matrix, AGG occurred as previously observed with the same amounts of the additives,³⁰ and basal grain boundaries formed between the abnormal and matrix grains, as seen in Fig. 2(b). Some matrix grains, however, formed curved grain boundaries with the large abnormal grain as indicated by an arrow in Fig. 2(c). The TEM micrograph of a basal grain boundary between an abnormal grain at the bottom and matrix grains at the top is shown in Fig. 3(a). The black arrows indicate the grain boundaries between the matrix grains intersecting the basal grain boundary.

In Fig. 2 the basal grain boundaries appeared to maintain their flat shape through the triple junctions containing grain boundaries between matrix grains. This flat shape of the basal grain boundary at a triple junction with a nearly vertical grain boundary is more clearly shown on the left of the circle A in a TEM micrograph of Fig. 3(a). The h&v structure on the right side of Fig. 3(a) would have appeared to be curved at the lower magnification in Fig. 2(c). The horizontal segments appeared to be basal grain boundaries, parallel to the (0001) plane of the large grain. The HRTEM images of the boundary segments in the circles marked A and B in Fig. 3(a) are shown in Figs. 3(b) and (c). The specimen was tilted to align the $[10\bar{1}0]$ zone axis of the large grain at the bottom to be nearly parallel to the beam, and the spacing between the horizontal planes in the bottom grains was about 4 Å, which was close to 4.33

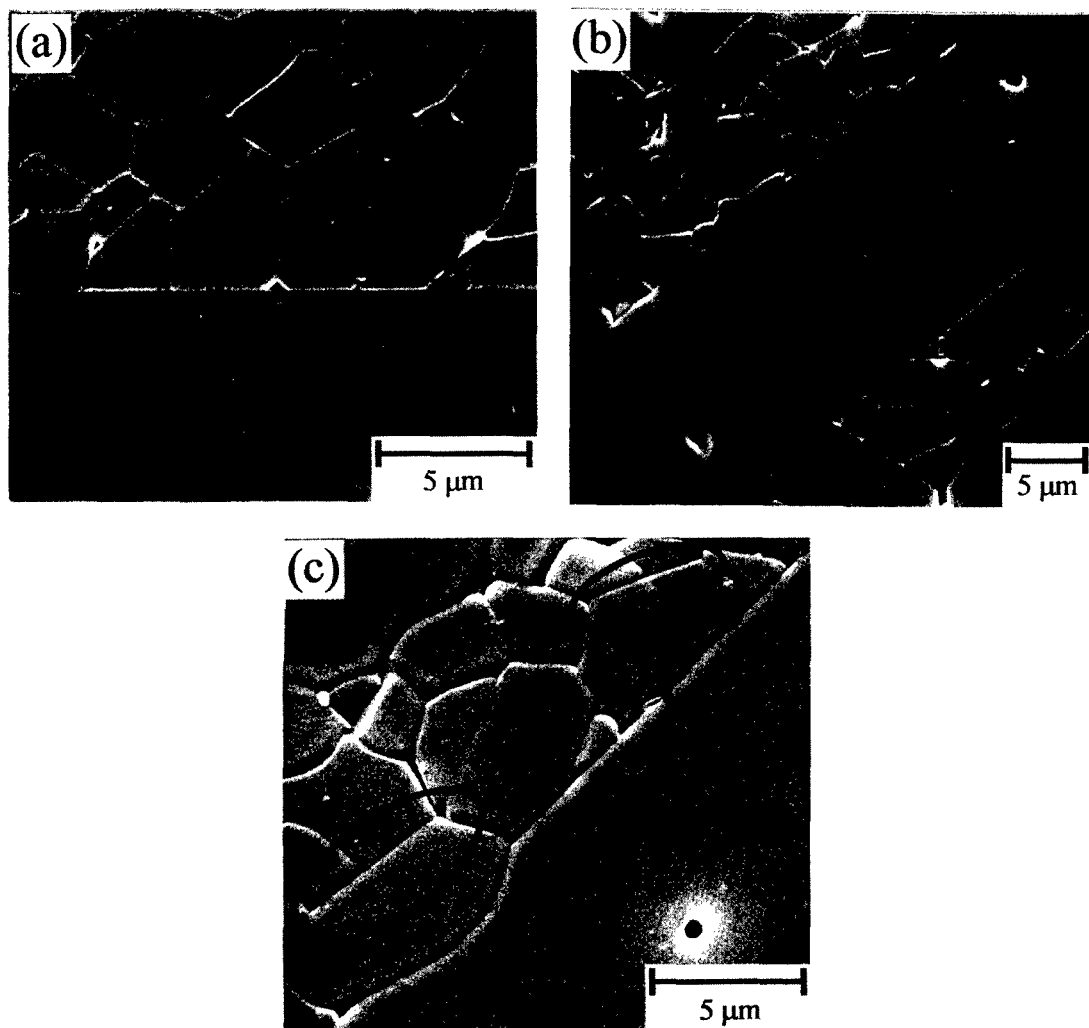


Fig. 2. SEM image of the microstructures of (a) the contact region between the (0001) face of a sapphire crystal and alumina powder with 100 ppm (by mole) of SiO_2 and 50 ppm of CaO sintered at 1620°C for 24 h, (b) the region with an abnormally large grain, and (c) another region between an abnormal grain and matrix grains at a higher magnification.

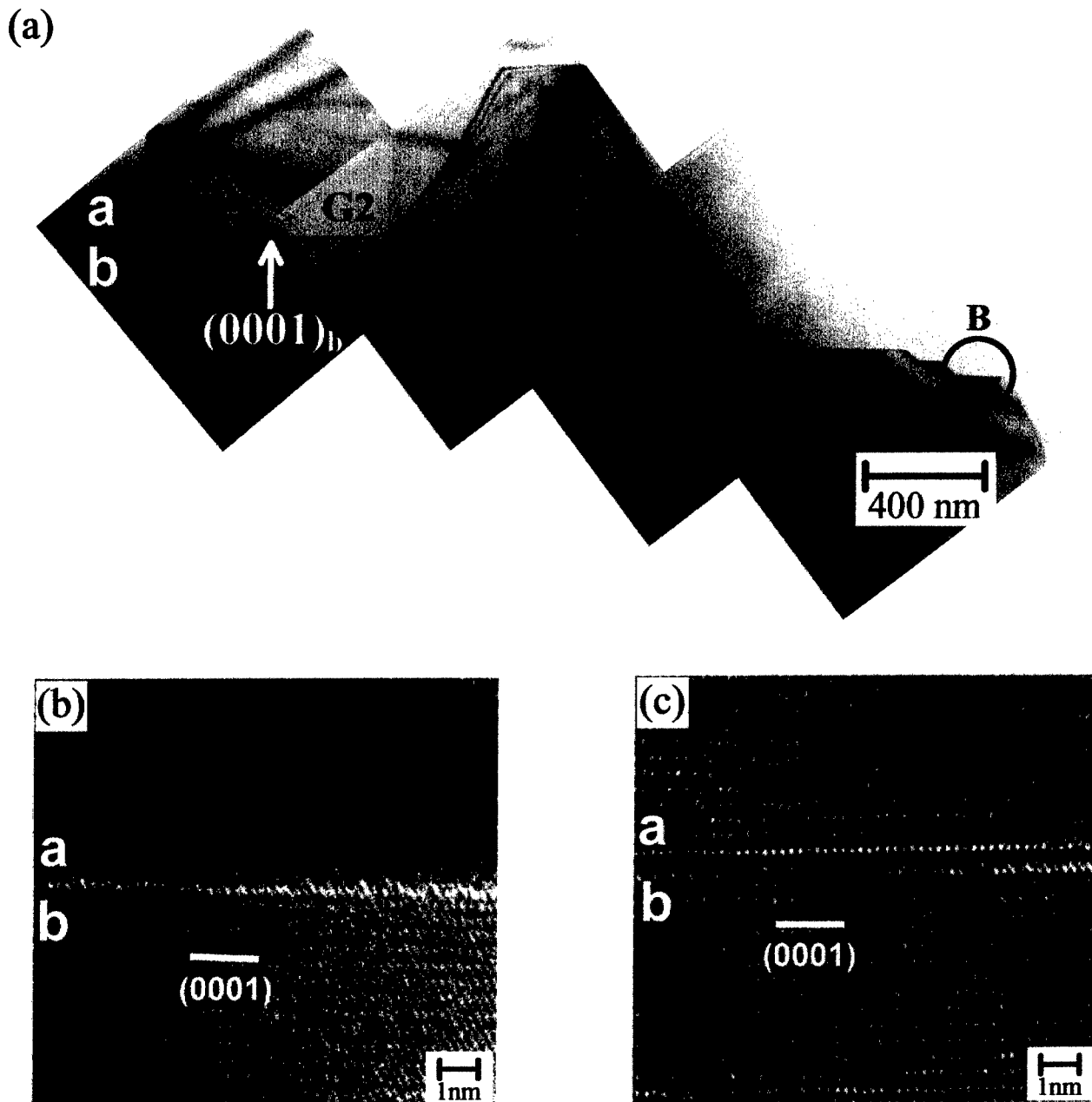


Fig. 3. (a) TEM image of the interface between the (0001) plane of a large abnormal grain (bottom) and small matrix grains in the specimen with 100 ppm (by mole) of SiO_2 and 50 ppm of CaO sintered at 1620°C for 24 h, and the HRTEM images (with $[10\bar{1}0]$ zone axis of the large grain) of the circled regions marked (b) A and (c) B in Fig. 3(a) (In (a), G1, G2, and G3 designate the grains meeting at the triple junction T for the schematic ξ -vector analysis of Fig. 4.)

Å for the spacing between the basal planes of alumina.³⁸ These HRTEM images confirmed that the flat grain boundaries and the horizontal segments of the h&v grain boundaries were indeed basal grain boundaries.

No pockets of an amorphous phase were observed at the triple junctions in Fig. 3(a) and the HRTEM images did not show any amorphous phase at these basal grain boundaries. Gülgün *et al.*³⁵ and Swiatnicki *et al.*³² also observed basal grain boundaries in alumina without any liquid phase. It thus appears that the concentrations of SiO_2 (100 ppm) and CaO (50 ppm) in our specimens were not high enough to form a liquid phase at 1620°C .³⁹

The flat shapes of these basal grain boundaries indicate that they are singular corresponding to cusps in the γ plots for grains embedded in other grains of various misorientation angles. If, and only if, they are singular, their flat shapes can be maintained at the

triple junctions with other grain boundaries. The equilibria at triple junctions can be analyzed by using the capillarity vectors (ξ -vectors) proposed by Hoffmann and Cahn.^{40,41} Three grain boundaries are in equilibrium at a triple junction if the projections of their ξ -vectors on a plane perpendicular to the junction add up to 0. The equilibrium shapes of the three grains in two dimensions, which will depend on the misorientation between the grain pairs, with both singular (flat) and rough (curved) grain boundaries, are schematically shown in Fig. 4. The shape of grain G1 is of that grain embedded in G2, and hence G1 is bound by the grain boundaries between G1 and G2. Likewise, G2 is bound by the grain boundaries between G2 and G3, and G3 is bound by the grain boundaries between G3 and G1. The grains G2 and G3 with parallel flat grain boundaries have a common center at C, and the triple junction is in equilibrium if the boundary of G1 intersects the

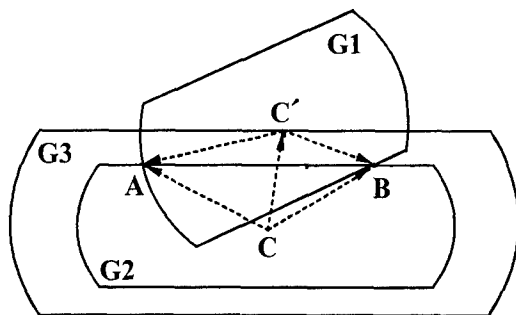


Fig. 4. Illustration of the equilibria at triple junctions of grains G1, G2, and G3 with parallel singular grain boundaries of G2 and G3. The dotted lines between C and C', C' and A (or B), and C and A (or B) are the ξ -vectors for grains G3, G1, and G2, respectively.

boundary of G2 as the center of G1 (indicated by C') moves along the flat boundary of G3. If, for example, the boundary of G1 intersects the boundary of G2 at the point A (or B), the dotted lines between C and C', C' and A (or B), and C and A (or B), which are the corresponding ξ -vectors, form a triangle. The triple junction equilibrium is thus possible with two extended flat (singular) boundaries if the third boundary is either singular or rough. If the third boundary (of G3) has an h&v shape, however, its ξ -vector is fixed at a corner of G3, and hence it will be nearly impossible to reach equilibrium at the triple junction. In such a case, the orientation of the third boundary near the triple junction may deviate from those appearing at the corners of the equilibrium shapes. If, on the other hand, a singular boundary (of G2) intersects an h&v boundary (of G3) with parallel singular segments as shown in Fig. 3(a) at the junction indicated by T, the third boundary (of G1) in equilibrium may be either rough or singular as can be seen by placing the center of G1 at a corner of G3 in Fig. 4.

If the boundaries of G1 and G2 are rough and hence their equilibrium shapes consist of only curved boundaries, it can be readily shown by a schematic analysis similar to Fig. 4 that their boundaries cannot meet at a triple junction with a contact angle of 180° . It can thus be concluded that the basal grain boundaries with their flat shapes extending through the triple junctions as shown in Figs. 3 and 4 are possible if and only if they are singular. Their properties are thus similar to those of the twin boundaries which maintain their flat shapes at the junctions with grain boundaries and surfaces. The flat grain boundaries extending through the triple junctions were also found between the matrix grains as indicated by the ellipses in Fig. 2(c). It is likely that these flat grain boundaries also lie on the basal planes of the larger grains.

In another series of experiments, an alumina single crystal was embedded in pure alumina powder and sintered identically to the specimen shown in Fig. 1. This sintered specimen was heat-treated again after packing in alumina powder with 100 ppm of SiO_2 and 50 ppm of CaO. The grain boundaries between the single crystal and the matrix grains, which were curved after the sintering treatment as shown in Fig. 1, became flat after the second heat treatment as shown in Fig. 5. Although there is some ambiguity arising from the slight movement of the boundary front toward the small grains, this result confirms the earlier conclusion that pure alumina grain boundaries are curved at all magnifications and hence rough, while with SiO_2 and CaO, singular basal grain boundaries form.

It is conceivable that the basal grain boundaries are produced by kinetic effects arising from their mobility decrease with the addition of SiO_2 and CaO. But basal grain boundaries were abundant in the relatively late stages of AGG when the grain boundary migration rates were fairly low because of large matrix grain size. Basal grain boundaries were also maintained between the large abnormal grains after their impingement,³⁰ when they are expected to be nearly immobile. It therefore appears that basal grain boundaries indeed represent the equilibrium shape.

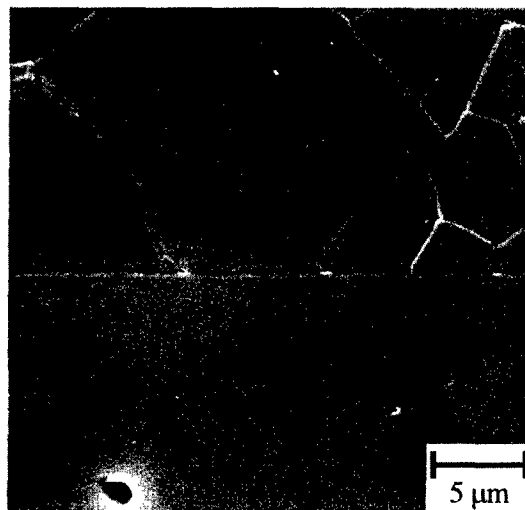


Fig. 5. SEM image of the contact region between the (0001) face of a sapphire crystal and pure alumina powder sintered at 1620°C for 24 h and heat-treated again after embedding in (alumina + 100 ppm SiO_2 + 50 ppm CaO) powder at 1620°C for 36 h.

If the grain boundaries between the basal planes of the large grains (either the sapphire single crystal or the large grain formed by AGG) and the neighboring small grains are singular, it is conceivable that singular grain boundaries can be formed between the basal planes of the small grains and high index planes of the large grains. Such a skewed boundary structure connecting the basal planes of the small grains will, however, have a higher boundary energy than the observed boundaries which are flat along the basal planes of the large grains, because the basal planes of the small grains have to be connected by boundary segments of high energy.

In addition to basal grain boundaries, Gülgün *et al.*³³ and Swiatnicki *et al.*³² observed flat grain boundaries with the rhombohedral $\{01\bar{1}2\}$ and other low index planes in one of the grain pairs. It thus appears that basal and other low index planes can form singular grain boundaries with almost any misorientation angles between the grains. This is consistent with the observation of h&v grain boundaries between the matrix grains, because some segments of these grain boundaries are likely to be low index singular boundaries. Low index grain boundaries have been frequently observed in both oxides and metals when attempts have been made to determine the boundary planes—in TiO_2 -excess BaTiO_3 ,⁴² Au,⁴³ MgAl_4O_7 -spinel,⁴⁴ Mo,⁴⁵ and Fe,⁴⁶ for example.

The computer simulations of Merkle and Wolf^{43,47} indicate that the grain boundary energy critically depends on the boundary normal and the cusps in the γ -plot can appear at inclination angles where one of the grains has a low index plane. But the heat-treatment atmosphere and additives have been observed to have strong effects on the formation of h&v and flat grain boundaries in Ni,¹⁵ Ag,⁴⁸ Cu (with Bi),^{18,19} Fe (with Te),^{49,50} BaTiO_3 (with TiO_2),⁴² and alumina (with SiO_2 and CaO).³⁰ Similar effects of additives on the equilibrium shapes of crystals in contact with vapor or liquid have also been observed in a number of systems.⁵¹⁻⁵⁴ As shown by the phenomenological theories of Gjostein⁵⁵ and Shewmon and Robertson,⁵⁶ these effects must arise from the changes of the boundary step free energy, but presently we do not understand why these additive species produce such changes.

As noted earlier in this report, in the specimen containing SiO_2 and CaO, some matrix grains formed apparently curved grain boundaries with the basal faces of the abnormal grains and sapphire crystals as indicated by an arrow in Fig. 2(c). These grain boundaries may in fact reveal h&v shapes at high magnifications as shown on the right side Fig. 3(a). The reasons for such a grain boundary shape are presently not clear. One possibility is that for certain misorientation angles between the grains, some basal grain boundaries have low mobilities and are therefore left behind

during the growth of the large grains. Or the cusp for this basal grain boundary may not be sufficiently deep to keep a flat shape.

In the final experiment of this work, a specimen sintered after doping with SiO_2 and CaO to obtain the structures shown in Figs. 2 and 3 was heat-treated again after packing in MgO powder. All the flat basal grain boundaries between the single crystal and the matrix grains and between the abnormal grains and the matrix grains obtained after sintering with SiO_2 and CaO became curved on exposure to MgO as shown in Fig. 6, resembling those of pure alumina shown in Fig. 1(a). The TEM observations confirmed the curved shapes of the grain boundaries between an abnormal grain and the matrix grains as shown in Fig. 7(a). The circled region A in Fig. 7(a) is shown in Fig. 7(b) at a higher magnification to confirm its curved shape. At this magnification, the grain boundaries between the matrix grains were also observed to be curved in agreement with our previous observation of a specimen with 100 ppm of SiO_2 , 50 ppm of CaO , and 600 ppm of MgO ³⁰ (In contrast, many grain boundaries between the small grains in the specimen with 100 ppm of SiO_2 and 50 ppm of CaO had h&v shapes when observed at approximately the same magnification.³⁰) An HRTEM image of the circled region B in Fig. 7(a) is shown Fig. 7(c). It confirmed the curved shape of this grain boundary even at atomic scale.

The curved shapes of the grain boundaries at all scales of observation indicate that they are atomically rough. For most of the grain-grain misorientations, the grain boundary Wulff shapes will be rounded without any sharp corners or edges where the boundary

normals change discontinuously. The defaceting transitions of the grain boundaries between the matrix grains are also consistent with this conclusion. These observations thus show that the basal grain boundaries and probably other singular grain boundaries underwent roughening transitions when MgO was added. The inverse transition from the rough to the singular grain boundaries was induced by adding SiO_2 and CaO to pure alumina as described earlier in this report.

The formation of the large grains with basal grain boundaries (as shown in Fig. 2(b)) during AGG in the specimens with SiO_2 and CaO indicate that these basal grain boundaries have very low energy. It is therefore likely that if these basal grain boundaries become rough by adding MgO , all other grain boundaries will also become rough as indeed indicated by the curved shapes of the grain boundaries between the matrix grains in Fig. 6. Previously, Kaysser *et al.*³¹ also observed that the grain boundaries between a sapphire and many small alumina grains in contact were all curved when 0.1 wt% MgO was added. But the impurity content in the alumina powder was unknown and the formation of a small amount of liquid phase could not be ruled out. If the grain boundaries become rough by MgO addition, their structures and energies will be more isotropic. This possibility is consistent with the observation by Handwerker *et al.*⁵⁷ that the distribution of the surface-grain boundary dihedral angles in alumina became narrower when MgO was added.

The HRTEM images of rough grain boundaries shown in Figs. 1(b) and 7(c) were observed after cooling (although rapidly) the

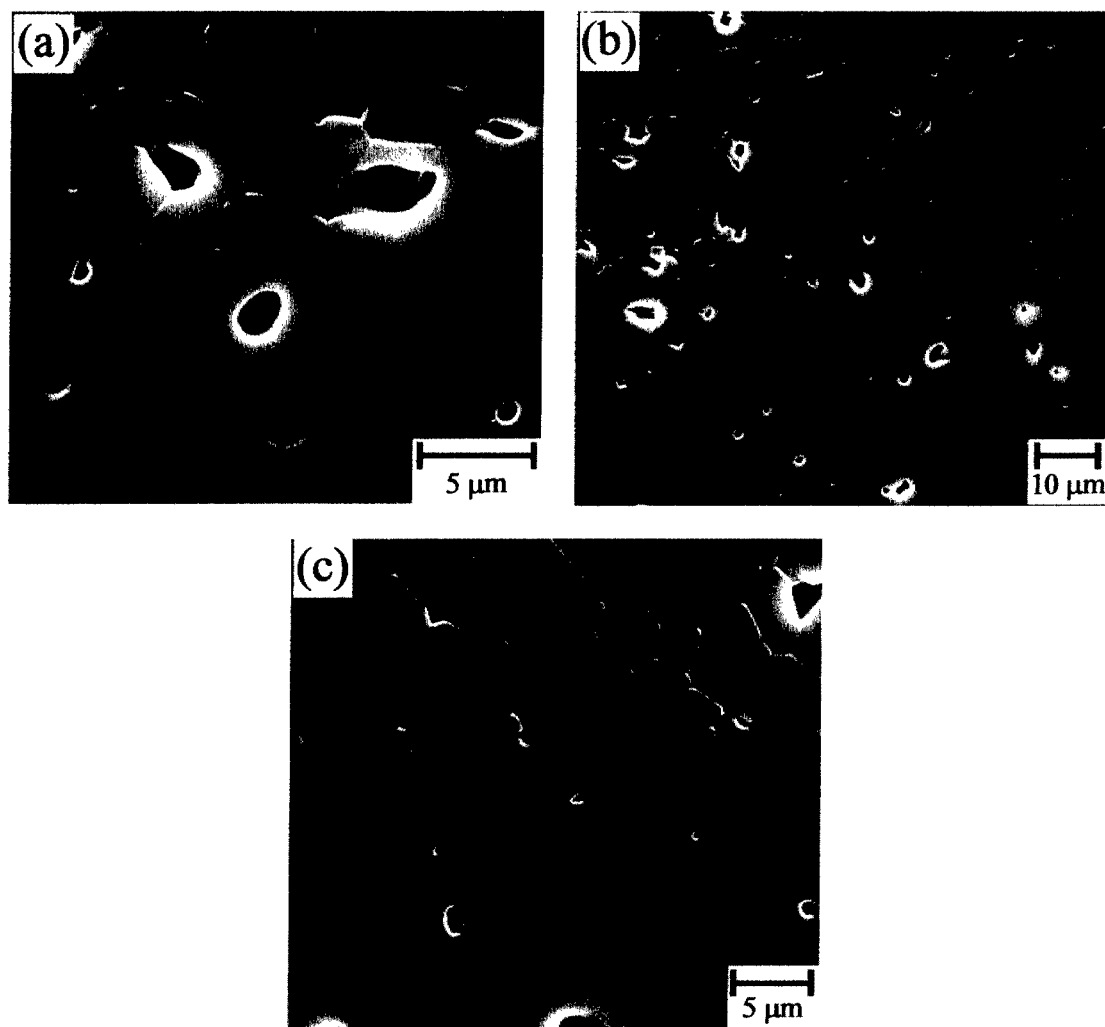


Fig. 6. SEM images of (a) the contact region between the (0001) face of a sapphire crystal and matrix grains, (b) the region with an abnormal grain, and (c) the region between an abnormal grain and matrix grains at a higher magnification in a specimen initially sintered at 1620°C for 24 h after adding 100 ppm of SiO_2 and 50 ppm of CaO and heat-treated again at 1620°C for 10 h after embedding in MgO powder.

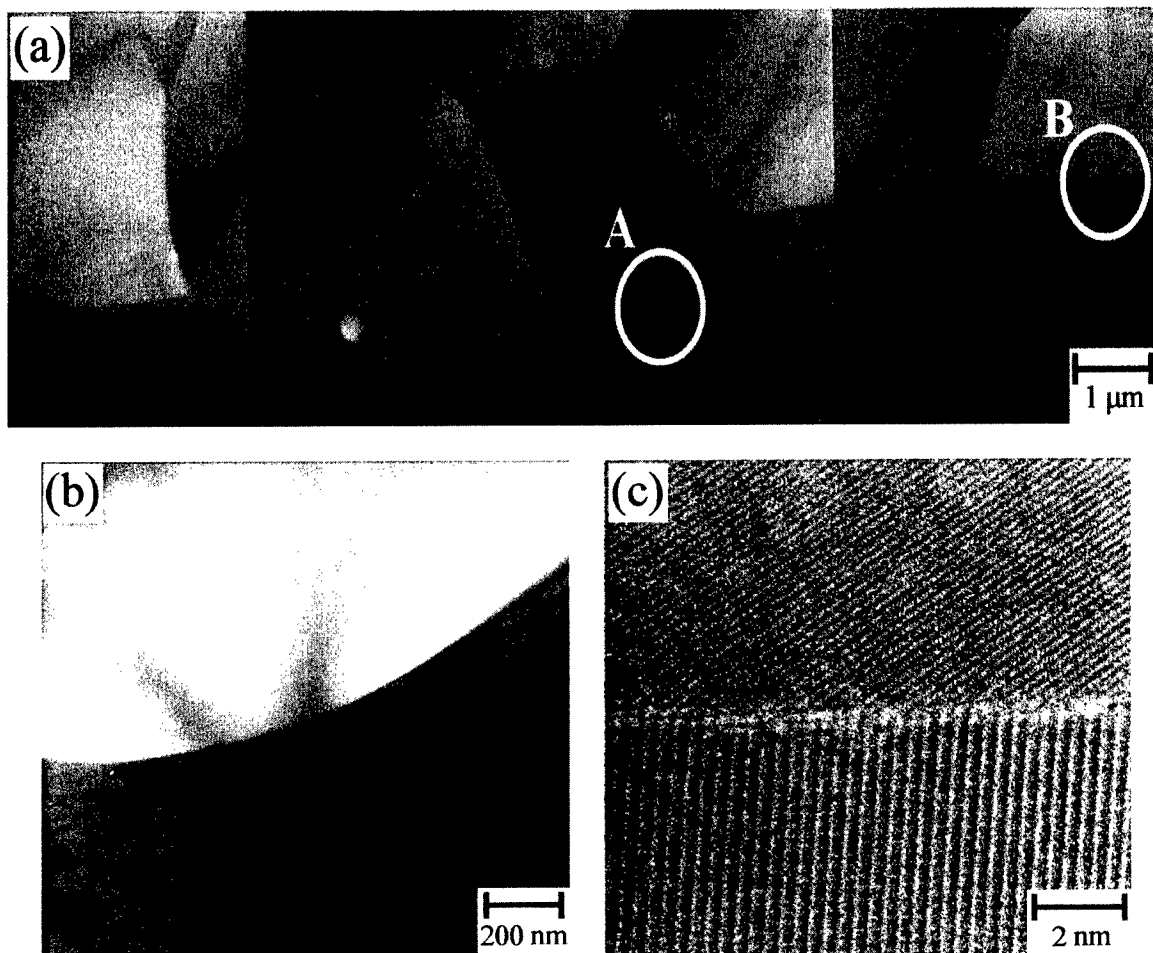


Fig. 7. TEM image of the microstructures of the same specimen as that shown in Fig. 6 of (a) grain boundaries between a large abnormal grain (bottom) and matrix grains (top), (b) the circled region A at a higher magnification, and (c) the circled region B under high-resolution conditions.

specimens to the room temperature. It is possible that at high temperatures such as 1620°C, their atomic structure is more disordered. Although these rough grain boundaries may undergo singular (faceting) transitions at low temperatures as in metals,^{15,17,48} the absence of any fine-scale h&v structures indicates that characteristics of their rough structures are retained during cooling. It is possible that the kinetic rate is very low because of low transition temperatures.

It was shown by scanning ion microprobe analysis that in polycrystalline alumina doped with 250 ppm MgO (by mole), both MgO and CaO strongly segregated at grain boundaries.⁵⁸ Although we do not yet understand why these segregating elements change the grain boundary structure, it is interesting to note that the additions of SiO₂, CaO, and MgO appear to produce the same effects on all types of interfaces in alumina. The interfaces between alumina grains and anorthite liquid were singular and became partially rough when MgO was added.⁵⁹ The faceted surfaces of alumina (with h&v structures) became defaceted and hence atomically rough when exposed to MgO vapor.⁹ Similarly, oxygen causes the faceting of both surfaces and grain boundaries in Ni¹⁵ and Ag,⁴⁸ and C in Ni causes defaceting of both surfaces and grain boundaries.¹⁵

The grain boundary roughening transition in alumina appears to be quite analogous to that observed in TiO₂-excess BaTiO₃.^{60,61} When heat-treated in air well below the eutectic temperature, abnormal grains grew along double twins, forming flat (111) grain boundaries with matrix grains, and the grain boundaries between the matrix grains were faceted with h&v shapes. When heat-treated in hydrogen, the initially flat (111) grain boundaries became curved and the grain boundaries between the small grains became defaceted.⁶⁰ Similar changes of the grain boundary structure were observed with changes in the amount of excess TiO₂.⁴²

The grain boundary roughening transition can produce large effects on the properties that depend on grain boundary structure.

In alumina,³⁰ BaTiO₃,⁶⁰ and several metals,^{15–17,48,62} it was observed that normal grain growth occurred with rough grain boundaries and abnormal grain growth with singular grain boundaries. Earlier, Lartigue and Priester⁶³ observed that sintered alumina showed AGG with the large grains elongated in their (0001) directions with flat (0001) grain boundaries. When MgO was added, normal grain growth occurred with equiaxial grains and curved grain boundaries. It appears that their alumina powder of 99.96% purity either contained initially or picked up during sintering some impurities to cause the formation of singular grain boundaries without MgO. The grain boundary roughening transition may also be related to the changes (with temperature or additives) in grain boundary sliding in Zn,²² Cu,²³ and Al,²⁴ creep in alumina doped with Y₂O₃ and MgO,^{64,65} grain boundary diffusion,^{66–68} and sintering.⁶⁹ The addition of Y₂O₃ and other oxides to alumina decreases the creep rate.^{64,65,70} and the addition of Y₂O₃ was also observed to cause AGG^{33,34,71,72} and produce basal grain boundaries.^{33,34} It is therefore possible that the creep rate is affected by the singular or roughening transition of the grain boundary.

IV. Conclusions

The results presented here show that, in pure alumina, the grain boundaries formed the (0001) surface of a sapphire single crystal and small matrix grains and between matrix grains are atomically rough. On adding SiO₂ and CaO, these grain boundaries became singular with flat shapes extending through the triple junctions. The abnormal grains also formed singular basal grain boundaries with matrix grains of randomly varying misorientations. On adding MgO these singular basal grain boundaries became rough. Although singular grain boundaries could also form with other low index planes as indicated by previous work, this

work was focused on the basal grain boundaries because they are naturally produced during AGG and could be readily identified from their flat shapes. It appears that with SiO₂ and CaO the basal grain boundaries have the deepest cusps in the γ -plots. Therefore, if the basal grain boundaries are rough, the other grain boundaries are also expected to be rough. To draw these conclusions about the atomic scale structures of these grain boundaries, the observations had to be made at all scales. The results of this work provide a further support for our earlier proposal³⁰ that the addition of MgO to alumina containing SiO₂ and CaO induces normal grain growth because the grain boundaries become rough. The same relationship between the grain boundary structure and grain growth was also found in Ni, Ag, a Ni-base superalloy, 316L stainless steel, and Ti-excess BaTiO₃.

References

- ¹W. K. Burton and N. Cabrera, "Crystal Growth and Surface Structure," *Discuss. Faraday Soc.*, **5**, 33–39 (1949).
- ²W. K. Burton, N. Cabrera, and F. C. Frank, "The Growth of Crystals and the Equilibrium Structure of Their Surfaces," *Philos. Trans. R. Soc. London, A*, **A243**, 299–358 (1951).
- ³F. C. Frank, "The Geometrical Thermodynamics of Surfaces"; pp. 1–15 in *Metal Surfaces: Structure, Energetics, and Kinetics*. American Society for Metals, Metals Park, OH, 1963.
- ⁴J. D. Weeks, "The Roughening Transition"; pp. 293–317 in *Ordering in Strongly Fluctuating Condensed Matter Systems*. Edited by T. Riste. Plenum, New York, 1980.
- ⁵H. van Beijeren and I. Nolden, "The Roughening Transition"; pp. 259–300 in *Structure and Dynamics of Surfaces II: Phenomena, Models, and Methods*. Edited by W. Schommers and P. von Blanckenhagen. Springer-Verlag, Berlin, Germany, 1987.
- ⁶M. Wortis, "Equilibrium Crystal Shapes and Interfacial Phase Transitions"; pp. 367–405 in *Chemistry and Physics of Solid Surfaces VII*. Edited by R. Vanselow and R. F. Howe. Springer-Verlag, Berlin, Germany, 1988.
- ⁷E. H. Conrad, "Surface Roughening, Melting, and Faceting," *Prog. Surf. Sci.*, **39**, 65–116 (1992).
- ⁸C. Herring, "Some Theorems on the Free Energies of Crystal Surfaces," *Phys. Rev.*, **82**, 87–93 (1951).
- ⁹C. W. Park and D. Y. Yoon, "Effect of Magnesium Oxide on Faceted Vicinal (0001) Surface of Aluminum Oxide," *J. Am. Ceram. Soc.*, **84** [2] 456–58 (2001).
- ¹⁰E. W. Hart, "Grain Boundary Phase Transformations"; pp. 155–70 in *The Nature and Behavior of Grain Boundaries*. Edited by H. Hu. Plenum Press, New York, 1972.
- ¹¹G. Ciccotti, M. Guillopé, and V. Pontikis, "High-Angle Grain-Boundary Premelting Transition: A Molecular-Dynamics Study," *Phys. Rev. B*, **27**, 5576–85 (1983).
- ¹²T. Nguyen, P. S. Ho, T. Kwok, C. Nitta, and S. Yip, "Grain-Boundary Melting Transition in an Atomistic Simulation Model," *Phys. Rev. Lett.*, **57**, 1919–22 (1986).
- ¹³C. Rottman, "Roughening of Low-Angle Grain Boundaries," *Phys. Rev. Lett.*, **57**, 735–38 (1986).
- ¹⁴T. E. Hsieh and R. W. Balluffi, "Observations of Roughening/De-faceting Phase Transitions in Grain Boundaries," *Acta Metall.*, **37**, 2133–39 (1989).
- ¹⁵S. B. Lee, N. M. Hwang, D. Y. Yoon, and M. F. Henry, "Grain Boundary Faceting and Abnormal Grain Growth in Nickel," *Metall. Mater. Trans. A*, **31A**, 985–94 (2000).
- ¹⁶S. B. Lee, D. Y. Yoon, and M. F. Henry, "Abnormal Grain Growth and Grain Boundary Faceting in a Model Ni-Base Superalloy," *Acta Mater.*, **48**, 3071–80 (2000).
- ¹⁷J. S. Choi and D. Y. Yoon, "The Temperature Dependence of Abnormal Grain Growth and Grain Boundary Faceting in 316L Stainless Steel," *ISIJ Int.*, **41**, 478–83 (2001).
- ¹⁸A. M. Donald and L. M. Brown, "Grain Boundary Faceting in Cu–Bi Alloys," *Acta Metall.*, **27**, 59–66 (1979).
- ¹⁹T. G. Ference and R. W. Balluffi, "Observation of a Reversible Grain Boundary Faceting Transition Induced by Changes of Composition," *Ser. Metall.*, **22**, 1929–34 (1988).
- ²⁰U. Dahmen and K. H. Westmacott, "Studies of Faceting by High Voltage/High Resolution Microscopy"; pp. 133–67 in *Interface: Structure and Properties*. Edited by C. S. Pande, B. B. Rath, and D. A. Smith. Trans Tech Publications, Uetikon-Zürich, Switzerland, 1993.
- ²¹L. S. Shvindlerman and B. B. Straumal, "Regions of Existence of Special and Non-special Grain Boundaries," *Acta Metall.*, **33**, 1735–49 (1985).
- ²²T. Watanabe, S.-I. Kimura, and S. Karashima, "The Effect of a Grain Boundary Structural Transformation on Sliding in (10 $\bar{1}0$)-Tilt Zinc Bicrystals," *Philos. Mag. A*, **49**, 845–64 (1984).
- ²³P. Lagarde and M. Biscondi, "Intercrystalline Creep of Oriented Copper Bicrystals," *Mem. Sci. Rev. Metall.*, **71**, 121–31 (1974).
- ²⁴P. Lagarde and M. Biscondi, "Fluage Intergranulaire de Bicristaux Symétriques de Flexion Autour de (001) dans l'Aluminium," *Can. Metall. Q.*, **13**, 245–51 (1974).
- ²⁵K. T. Aust, "Interface Migration"; pp. 307–34 in *Interfaces Conference, Melbourne*. Edited by R. C. Gifkins. Australian Institute of Metals, Butterworth, London, U.K., 1969.
- ²⁶C. Rottman and M. Wortis, "Statistical Mechanics of Equilibrium Crystal Shapes: Interfacial Phase Diagrams and Phase Transitions," *Phys. Rep.*, **103**, 59–79 (1984).
- ²⁷S. I. Bae and S. Baik, "Determination of Critical Concentrations of Silica and/or Calcium for Abnormal Grain Growth in Alumina," *J. Am. Ceram. Soc.*, **76** [4] 1065–67 (1993).
- ²⁸J. Bae and S. Baik, "Abnormal Grain Growth of Alumina," *J. Am. Ceram. Soc.*, **80** [5] 1149–56 (1997).
- ²⁹C. A. Bateman, S. J. Bennisson, and M. P. Harmer, "Mechanism for the Role of Magnesia in the Sintering of Alumina Containing Small Amounts of a Liquid Phase," *J. Am. Ceram. Soc.*, **72** [7] 1241–44 (1989).
- ³⁰C. W. Park and D. Y. Yoon, "Effects of SiO₂, CaO, and MgO Additions on the Grain Growth of Alumina," *J. Am. Ceram. Soc.*, **83** [10] 2605–609 (2000).
- ³¹W. A. Kaysser, M. Sprissler, C. A. Handwerker, and J. E. Blendell, "Effect of a Liquid Phase on the Morphology of Grain Growth in Alumina," *J. Am. Ceram. Soc.*, **70** [5] 339–43 (1987).
- ³²W. Swiatnicki, S. Lartigue-Korinek, and J. Y. Laval, "Grain Boundary Structure and Intergranular Segregation in Al₂O₃," *Acta Metall. Mater.*, **43**, 795–805 (1995).
- ³³M. A. Gülgün, V. Putlayev, and M. Rühle, "Effects of Yttrium Doping α -Alumina: I. Microstructure and Microchemistry," *J. Am. Ceram. Soc.*, **82** [7] 1849–56 (1999).
- ³⁴S. Lartigue, L. Priester, F. Dupau, P. Gruffel, and C. Carry, "Dislocation Activity and Differences between Tensile and Compressive Creep of Yttria Doped Alumina," *Mater. Sci. Eng. A*, **A164**, 211–15 (1993).
- ³⁵S. J. Bennisson and M. P. Harmer, "Grain-Growth Kinetics for Alumina in the Absence of a Liquid Phase," *J. Am. Ceram. Soc.*, **68** [1] C-22–C-24 (1985).
- ³⁶S. I. Bae and S. Baik, "Sintering and Grain Growth of Ultrapure Alumina," *J. Mater. Sci.*, **28**, 4197–204 (1993).
- ³⁷C. A. Handwerker, P. A. Morris, and R. L. Coble, "Effects of Chemical Inhomogeneities on Grain Growth and Microstructure in Al₂O₃," *J. Am. Ceram. Soc.*, **72** [1] 130–36 (1989).
- ³⁸M. L. Kronberg, "Plastic Deformation of Single Crystals of Sapphire: Basal Slip and Twinning," *Acta Metall.*, **5**, 507–24 (1957).
- ³⁹E. M. Levin, C. R. Robbins, and H. F. McMurdie; pp. 219–20 in *Phase Diagrams for Ceramists*, Vol. 1. Edited by M. K. Reser. American Ceramic Society, Columbus, OH, 1964.
- ⁴⁰D. W. Hoffman and J. W. Cahn, "A Vector Thermodynamics for Anisotropic Surfaces," *Surf. Sci.*, **31**, 368–88 (1972).
- ⁴¹J. W. Cahn and D. W. Hoffman, "A Vector Thermodynamics for Anisotropic Surfaces. II. Curved and Faceted Surfaces," *Acta Metall.*, **22**, 1205–14 (1974).
- ⁴²T. Yamamoto, Y. Ikuhara, K. Hayashi, and T. Sakuma, "Grain Boundary Structure in TiO₂-Excess Barium Titanate," *J. Mater. Res.*, **13**, 3449–52 (1998).
- ⁴³K. L. Merkle and D. Wolf, "Low-Energy Configurations of Symmetric and Asymmetric Tilt Grain Boundaries," *Philos. Mag. A*, **65**, 513–30 (1992).
- ⁴⁴C. B. Carter, " $\Sigma = 99$ and $\Sigma = 41$ Grain Boundaries," *Acta Metall.*, **36**, 2753–60 (1988).
- ⁴⁵J.-M. Penisson, "Atomic Structure of Tilt Boundaries in Mo Bicrystals," *J. Phys. Colloq.*, **49**, C5–87–C5–97 (1988).
- ⁴⁶H. Ichinose and Y. Ishida, "High Resolution Electron Microscopy of Grain Boundaries in FCC and BCC Metals," *J. Phys. Colloq.*, **46**, C4–39–C4–49 (1985).
- ⁴⁷D. Wolf and K. L. Merkle, "Correlation between the Structure and Energy of Grain Boundaries in Metals"; pp. 87–150 in *Materials Interfaces*. Edited by D. Wolf and S. Yip. Chapman and Hall, London, U.K., 1992.
- ⁴⁸J. B. Koo and D. Y. Yoon, "The Dependence of Normal and Abnormal Grain Growth in Silver on Annealing Temperature and Atmosphere," *Metall. Mater. Trans. A*, **32A**, 469–75 (2001).
- ⁴⁹J. R. Rellick, C. J. McMahon Jr., H. L. Marcus, and P. W. Palmberg, "The Effect of Tellurium on Intergranular Cohesion in Iron," *Metall. Trans.*, **2**, 1492–94 (1971).
- ⁵⁰C. Pichard, J. Rieu, and C. Goux, "Influence des Impuretés Métalloïdiques de la Famille du Soufre sur la Fragilité Intergranulaire du fer Pur," *Mem. Sci. Rev. Metall.*, **70**, 13–22 (1973).
- ⁵¹B. E. Sundquist, "A Direct Determination of the Anisotropy of the Surface Free Energy of Solid Gold, Silver, Copper, Nickel, and Alpha and Gamma Iron," *Acta Metall.*, **12**, 67–86 (1964).
- ⁵²B. E. Sundquist, "The Effect of Metallic Impurities and Temperature on the Surface Free Energy of Solid Metals," *Acta Metall.*, **12**, 585–92 (1964).
- ⁵³J. Y. Jun, "Grain Shape and Abnormal Grain Growth in NbC–Fe"; M.S. Thesis. Department of Inorganic Materials Engineering, Seoul National University, Seoul, Korea, 1994.
- ⁵⁴J. H. Choi, "Effects of Carbon on the Grain Growth Behavior in TaC–Ni"; M.S. Thesis. Department of Materials Science and Engineering, Korea Advanced Institute of Science and Technology, Taejeon, Korea, 1997.
- ⁵⁵N. A. Gjostein, "Adsorption and Surface Energy (I): The Effect of Adsorption on the γ -Plot," *Acta Metall.*, **11**, 957–67 (1963).
- ⁵⁶P. G. Shewmon and W. M. Robertson, "Variation of Surface Tension with Orientation"; pp. 67–98 in *Metal Surfaces: Structure, Energetics, and Kinetics*. American Society for Metals, Metals Park, OH, 1963.
- ⁵⁷C. A. Handwerker, J. M. Dynys, R. M. Cannon, and R. L. Coble, "Dihedral Angles in Magnesia and Alumina: Distributions from Surface Thermal Grooves," *J. Am. Ceram. Soc.*, **73** [5] 1371–77 (1990).
- ⁵⁸K. K. Soni, A. M. Thompson, M. P. Harmer, D. B. Williams, J. M. Chabala, and R. Levi-Setti, "Solute Segregation to Grain Boundaries in MgO-Doped Alumina," *Appl. Phys. Lett.*, **66** [21–22] 2795–97 (1995).
- ⁵⁹C. W. Park and D. Y. Yoon, "Abnormal Grain Growth in Alumina with Anorthite Liquid and the Effect of MgO Addition," *J. Am. Ceram. Soc.*, **85** [6] 1585–93 (2002).
- ⁶⁰B.-K. Lee, S.-Y. Chung, and S.-J. L. Kang, "Grain Boundary Faceting and Abnormal Grain Growth in BaTiO₃," *Acta Mater.*, **48**, 1575–80 (2000).
- ⁶¹S. B. Lee, S.-Y. Choi, S.-J. L. Kang, and D. Y. Yoon, *J. Am. Ceram. Soc.*, submitted.
- ⁶²G.-H. Lee, J. S. Choi, and D. Y. Yoon, "The Dependence of Abnormal Grain Growth on Initial Grain Size in 316L Stainless Steel," *Z. Metallkd.*, **92**, 655–62 (2001).
- ⁶³S. Lartigue and L. Priester, "Influence of Doping Elements on the Grain Boundary Characteristics in Alumina," *J. Phys. Colloq.*, **49**, C5-451–C5-456 (1988).

⁶⁴J. D. French, J. Zhao, M. P. Harmer, H. M. Chan, and G. A. Miller, "Creep of Duplex Microstructures," *J. Am. Ceram. Soc.*, **77** [11] 2857–65 (1994).

⁶⁵J. Cho, M. P. Harmer, H. M. Chan, J. M. Rickman, and A. M. Thompson, "Effect of Yttrium and Lanthanum on the Tensile Creep Behavior of Aluminum Oxide," *J. Am. Ceram. Soc.*, **80** [4] 1013–17 (1997).

⁶⁶A. N. Aleshin, S. I. Prokofjev, and L. S. Shvindlerman, "Evidence of Structure Transformation in $\Sigma = 5$ Near-Coincidence Grain Boundaries," *Scr. Metall.*, **19**, 1135–40 (1985).

⁶⁷A. N. Aleshin, B. S. Bokstein, A. L. Petelin, and L. S. Shvindlerman, "Individual Twist Boundary Zinc Diffusion in Aluminium," *Metallofizika*, **2**, 83–89 (1980).

⁶⁸A. N. Aleshin, B. S. Bokstein, and L. S. Shvindlerman, "Diffusion of Zinc along (100) Tilt Boundaries in Aluminum," *Fizika Tverd. Tela*, **19**, 3511–15 (1977).

⁶⁹N. M. Hwang, Y. J. Park, D.-Y. Kim, and D. Y. Yoon, "Activated Sintering of Nickel-Doped Tungsten: Approach by Grain Boundary Structural Transition," *Scr. Mater.*, **42**, 421–25 (2000).

⁷⁰T. Sakuma, Y. Ikuhara, T. Yamamoto, and H. Yoshida, "Towards Grain Boundary Engineering in Advanced Ceramics"; in Proceedings of the 7th Japan-France Materials Science Seminar (JFMSS-7), Edited by T. Watanabe and J. Petit, in press.

⁷¹A. M. Thompson, K. K. Soni, H. M. Chan, M. P. Harmer, D. B. Williams, J. M. Chabala, and R. Leve-Setti, "Dopant Distributions in Rare-Earth-Doped Alumina," *J. Am. Ceram. Soc.*, **80** [2] 373–76 (1997).

⁷²C. M. Wang, G. S. Cargill III, H. M. Chan, and M. P. Harmer, "Structural Features of Y-Saturated and Supersaturated Grain Boundaries in Alumina," *Acta Mater.*, **48**, 2579–91 (2000). □